

FORMATION AND PARTICLE GROWTH OF TiO₂ IN SILICA XEROGEL GLASS CERAMIC DURING A SINTERING PROCESS

H. Aripin^{1*}, I Made Joni², Seitaro Mitsudo³, I Nyoman Sudiana⁴, Edvin Priatna¹,
Nundang Busaeri¹, Svilen Sabchevski⁵

¹*Department of Electrical Engineering, Faculty of Engineering, Siliwangi University, Tasikmalaya West Java 46115, Indonesia*

²*Nano Technology and Graphene Research Center (NTGRC), Padjadjaran University, Bandung, West Java 45363, Indonesia*

³*Research Center for Development of Far Infrared Region (FIR Center), University of Fukui, Fukui, Bunkyo,3-9-1, Fukui Prefecture 910-8507, Japan*

⁴*Department of Physics, Faculty of Mathematics and Natural Sciences, University of Haluoleo, Kendari, Southeast Sulawesi 93132, Indonesia*

⁵*Laboratory of Plasma Physics and Engineering, Institute of Electronics of the Bulgarian Academy of Sciences, 72, Tzarigradsko chaussee blvd, 1784-Sofia, Bulgaria*

(Received: October 2016 / Revised: June 2017 / Accepted: November 2017)

ABSTRACT

This investigation presents the synthesis procedure and the results of an investigation of the crystallite growth of TiO₂ and the formation of Si–O–Ti bonds in novel silica xerogel (SiO₂) glass ceramic produced from an amorphous SX derived from sago waste ash. The composition had been prepared by adding various amounts of TiO₂, from 20 wt% to 80 wt%, into the amorphous SiO₂, and then a series of samples were sintered at 1200°C for 2 hours. The influence of the content of TiO₂ and the sintering temperature on the properties of TiO₂, namely crystallite size and formation of Si–O–Ti bonds, has been studied in detail. The properties of the produced ceramics have been characterized on the basis of the experimental data obtained using X-ray diffraction (XRD) and Fourier transform infrared (FTIR) spectroscopy. It has been found that an addition of SiO₂ confers an appreciable effect on the quantity of Si–O–Ti bonds. The interpretation of the XRD pattern allows one to explain the increase in the crystallite size of rutile TiO₂ by a decreased quantity of Si–O–Ti bonds.

Keywords: Composite of TiO₂-SiO₂; Crystallite size; Silica xerogel; Si–O–Ti bond; Rutile TiO₂; TiO₂

1. INTRODUCTION

The composite of TiO₂-SiO₂ is an important engineering material that has numerous uses in various industrial applications. Among them are those related to the production of optical materials with a wide range of refractive indices (Wang et al., 1999; Chen et al., 2003), materials for photocatalysis (Aziz & Sofyan, 2009; Arun et al., 2012), and sensors with a high surface hydroxyl group and surface area (Shumaila et al., 2015), as well as dielectric materials with a very low leakage current and high dielectric constant (Vishwas et al., 2011). A promising and actively studied variety of the latter is the dielectric material used for high energy density capacitors, which is characterized by the absence of phase separation of SiO₂ and TiO₂ in the

*Corresponding author's email: aripin@unsil.ac.id, Tel: +62- 265-330634, Fax: +62- 265-330634
Permalink/DOI: <https://doi.org/10.14716/ijtech.v8i8.750>

composite.

Many studies have been carried out in order to investigate the properties of the TiO₂-SiO₂ composite using a variety of different process conditions, such as temperature, time, composition, and starting materials. It is important to control these conditions in order to avoid any structural changes that influence the formation and particle growth of TiO₂ in the composite. Nilchi et al. (2011) have studied the particle size, Brunauer-Emmett-Teller surface area, and phase transformation from anatase to rutile of the TiO₂-SiO₂ composite during the sintering process. It has been found that the TiO₂-SiO₂ composite has a crystalline anatase phase at around 300 °C and a rutile phase at high temperatures in the range of 600°C to 1100°C. The specific surface area decreases from 707.59 m²/g to 13.72 m²/g and the size of the anatase crystallites increases from 5.0 nm to 26.7 nm when the calcination temperature increases from room temperature to 1100°C. Mahyar et al. (2010) have prepared TiO₂-SiO₂ composites with a varying content of SiO₂. At a temperature of 500°C, the size of the anatase crystallites decreases from 11.4 nm to 6.7 nm and the specific surface area increases from 46.87 m²/g to 106.13 m²/g when the content of SiO₂ increases from 20 wt% to 50 wt%. Yang et al. (2005) have studied a film of the TiO₂-SiO₂ composite with various SiO₂:TiO₂ compositions. It has been found that the quantity of Si–O–Ti bonds increases, and at 700°C, the porosity decreases when the content of SiO₂ increases. These studies have demonstrated that the formation of the Ti–O–Si bond and amorphous SiO₂ in the TiO₂-SiO₂ composite could effectively increase the stability of anatase TiO₂, limit the growth of crystallites, and increase the surface area. The high quantity of Si–O–Ti bonds and the larger surface area facilitate the mass transfer of reactants, such as oxygen, and reaction intermediates; this improves the electrochemical activity in the high energy density capacitors (Marinela et al., 2013). In this case, SiO₂ has an important role in helping to create new catalytic sites and to obtain a large surface area, as well as a suitable porous structure (Riazian et al., 2011).

In previous studies, as has already been mentioned above, SiO₂ has been prepared from synthetic sources, such as tetraethoxysilane (TEOS) and tetramethylorthosilica (TMOS), as a precursor. The TEOS and TMOS as organic precursors, however, have demonstrated several of their disadvantages. They are rather expensive and highly toxic, and the fumes of TMOS can cause blindness. Therefore, SiO₂ production from these sources on an industrial scale is not technologically or economically viable. In our study, SiO₂ in the form of silica xerogel was prepared using a sago waste ash (Aripin et al., 2011; Aripin et al., 2012) as a starting powder and was used to produce TiO₂-SiO₂ composites by mixing 20 wt% and 40 wt% of TiO₂ into SiO₂ (Aripin et al., 2016). It was found that, at 900°C, the size of the anatase crystallites are 26.3 nm and 21.4 nm for 20 wt% and 40 wt% of TiO₂, respectively. In the present work, we have studied the effects of temperature and the expanded content of TiO₂ on the quantity of Si–O–Ti bonds and their relationship to the size of the rutile crystallites.

2. METHODS

2.1. Silica Xerogel and TiO₂ Composite Preparation

Amorphous silica xerogel (SiO₂) was extracted from sago waste (solid residue, which is left behind after the starch has been washed out) obtained from the sago processing plant in Kendari, Indonesia. The detailed extraction procedures are described elsewhere (Affandi et al., 2009; Aripin et al., 2011; Aripin et al., 2016). High-purity amorphous silica amounting to 98.8% has been observed (Aripin et al., 2011). Table 1 shows the chemical composition of the prepared powder samples using crystalline TiO₂ powder and silica xerogel. The sample of silica xerogel/TiO₂ with a chemical composition of 20 wt% TiO₂ (S20T) was prepared by dissolving 5 g of TiO₂ in a solution containing 50 mL ethanol and 50 mL deionized water, and then was stirred at 80°C for one hour. Next, 15 g of the silica xerogel powder was added slowly into the

solution containing Ti^{2+} ions under continuous stirring at 50°C for 6 hours. The pH factor of the mixed solution was adjusted to a value of 2.8 in order to obtain a white precipitate of Ti-hydroxide. The mixed solution was heated at 80°C until the solvent completely evaporated. The resultant $\text{TiO}_2\text{-SiO}_2$ powder was dried in an oven at a temperature of 120°C for 2 hours and then stored in a desiccator for a further treatment. The samples S40T, S60T and S80T were prepared following the same procedure.

Table 1 Chemical composition of samples of the synthesized $\text{TiO}_2\text{-SiO}_2$ composites

| Sample | Silica xerogel (g) | TiO_2 (g) |
|------------------------------|--------------------|--------------------|
| 20 wt% TiO_2 (S20T) | 5 | 15 |
| 40 wt% TiO_2 (S40T) | 8 | 12 |
| 60 wt% TiO_2 (S60T) | 12 | 8 |
| 80 wt% TiO_2 (S80T) | 16 | 4 |

2.2. Sintering the Synthesized $\text{TiO}_2\text{-SiO}_2$ Composites

The powder samples were placed into a porcelain crucible and then inserted into a horizontal furnace, where they were sintered with a controlled heating rate of $10^\circ\text{C}/\text{min}$ up to the temperature of 1200°C in air. Then the temperature was kept constant at 1200°C for 2 hours. The cooling was performed by natural convection after turning off the electric furnace and leaving the samples inside.

2.3. Method for Characterization of the Synthesized $\text{TiO}_2\text{-SiO}_2$ Composites.

In this study, X-ray diffraction (XRD) was used to determine the phases of the sample using a Smartlab X-ray diffractometer with filtered Cu $K\alpha$ radiation at a wavelength of 0.15418 nm. The accelerating voltage and the applied current were 40 kV and 30 mA, respectively. The diffraction patterns were registered over the 2θ range from 10° to 90° at a scan rate of $0.01^\circ/\text{s}$. Fourier transform infrared (FTIR) spectra were obtained using a Varian 800 FTIR spectrometer (Scimitar Series model) in the wavenumber range of $400\text{--}4000\text{ cm}^{-1}$ with a spectral resolution of 4 cm^{-1} . All FTIR measurements were carried out at room temperature in a specular reflectance mode using the KBr pellet technique.

3. RESULTS AND DISCUSSION

Figure 1 shows the XRD patterns of silica xerogel loaded with different amounts of TiO_2 and sintered at 1200°C . It can be seen that, in samples of 20–80 wt%, there is a peak at about $2\theta = 20.1^\circ$, which is related to the (220) plane of SiO_2 tridymite (T) (JCPDS 46-1045) (Xue et al., 2015). The other peaks are also observed at $2\theta = 20.9^\circ$, 27.5° , and 31.0° , which correspond to the (101), (111), and (101) planes of characteristic peaks for SiO_2 cristobalite (C) (JCPDS 39-1425) (Xue et al., 2015). The crystallization of cristobalite in the $\text{TiO}_2\text{-SiO}_2$ composite at 1200°C is related to thermodynamic factors. It has been reported that the standard enthalpy of formation for individual TiO_2 and SiO_2 is -519.7 kJ/mol and -910.7 kJ/mol , and the standard free energy change for individual TiO_2 and SiO_2 is -495.0 kJ/mol and -856.3 kJ/mol (CRC, 2006). Based on the aforementioned thermodynamic considerations, the crystallization of cristobalite requires a very large amount of energy, which may be provided at high temperature. Furthermore, in all samples, some peaks appear at $2\theta = 27.3^\circ$, 35.8° , 40.9° , 54.5° , 56.3° , 62.3° , 63.6° , 68.7° , and 68.9° . These peaks correspond to the (110), (101), (111), (211), (220), (002), (311), (301), and (112) planes of the rutile TiO_2 (R) (JCPDS 21-1276, 1997). This result is in agreement with the findings of the study of phase formation of TiO_2 xerogel composites carried out by Syhrial et al. (2016). As more TiO_2 is loaded, the intensity of the diffraction peaks in the tridymite and cristobalite decreases and the peak intensity of rutile increases.

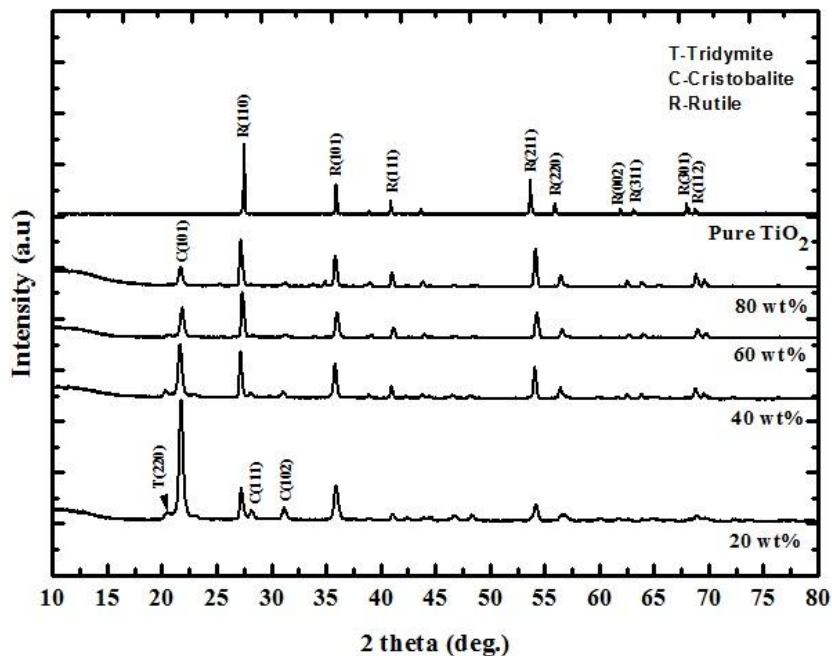


Figure 1 XRD patterns of TiO₂-SiO₂ composites with different amount of TiO₂, sintered at 1200°C

Figures 2 and 3 show the XRD patterns of the TiO₂-SiO₂ composites with 20 wt% and 40 wt% TiO₂, respectively, sintered at different temperatures. It can be seen that, in samples of 20 wt% and 40 wt% sintered at 900°C, a peak is exhibited at about $2\theta = 22.9^\circ$, which is related to the (101) plane of characteristic peaks for SiO₂ cristobalite (C). In the same samples, other peaks appear at $2\theta = 25.4^\circ, 37.8^\circ, 48.0^\circ, 53.7^\circ,$ and 54.5° , respectively. These peaks correspond to the (101), (004), (200), (105), and (211) planes of the SiO₂ anatase phase (A) (JCPDS 21-1272, 1997). These findings are in agreement with the results for TiO₂ nanoparticles derived from TiO₂-polymethyl methacrylate nanocomposites (Yuwono et al., 2010). TiO₂ rutile phases are also present in composites with 20 wt% and 40 wt% TiO₂. These phases appear at $2\theta = 27.3^\circ, 35.8^\circ, 40.9^\circ, 54.5^\circ,$ and 56.3° , which correspond to the (110), (101), (111), (211), and (220) planes, respectively (JCPDS 21-1276, 1997). It can also be seen that the intensity of the anatase and rutile phases appears to be higher for the samples loaded with 40 wt% TiO₂ than those of the samples with 20 wt% TiO₂, due to the smaller inclusion of amorphous silica xerogel.

Additionally, it was found that the TiO₂ phases exhibit a transformation from anatase to rutile as the sintering temperature increases for both samples. At 1200°C, a new peak of SiO₂ tridymite occurs at $2\theta = 20.1^\circ$. In addition, the anatase phase disappears completely and, eventually, it is replaced by a single phase of rutile; this occurs because the anatase phase is not stable at such a high temperature. At 1400°C, the SiO₂ tridymite and TiO₂ rutile peaks become sharper. An increase in rutile peaks indicates that the higher sintering temperature promotes the formation of rutile TiO₂ of high crystallinity. This phase transformation can be affected by SiO₂, which can improve the thermal stability of anatase phases, suppress the particle aggregation and grain growth of the anatase phase, and increase the specific area of the rutile phase.

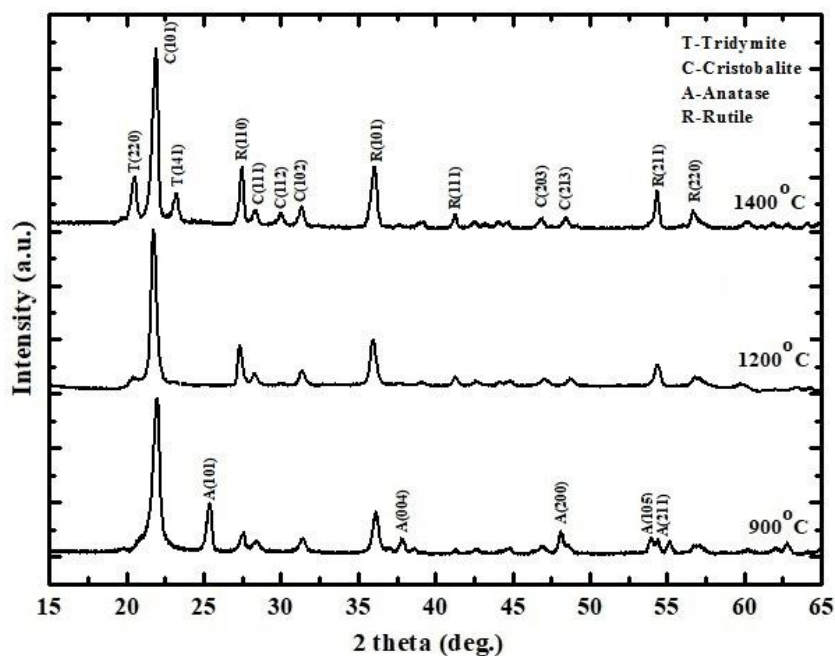


Figure 2 XRD patterns of $\text{TiO}_2\text{-SiO}_2$ composite with 20 wt% TiO_2 , sintered at different temperatures

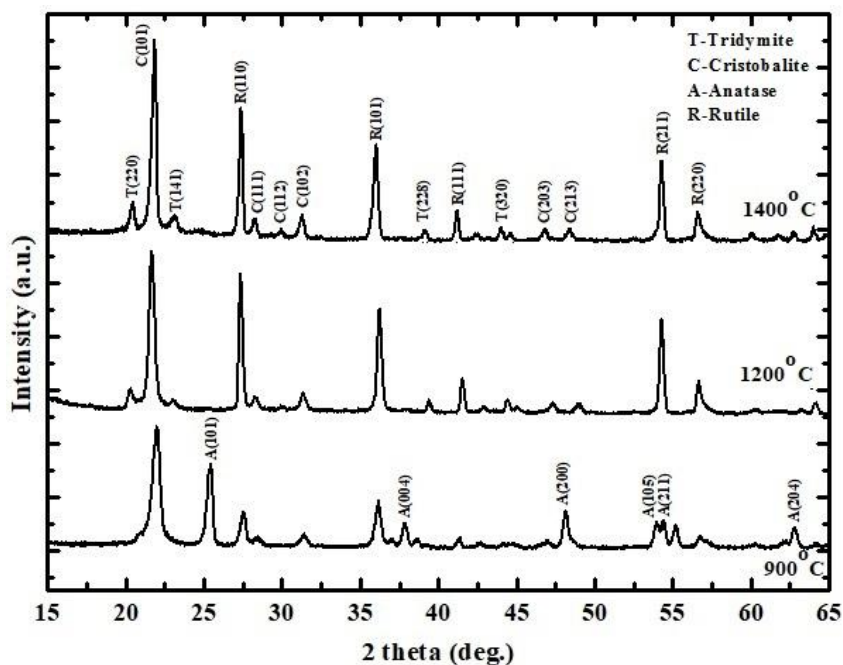


Figure 3 XRD patterns of $\text{TiO}_2\text{-SiO}_2$ composite with 40 wt% TiO_2 , sintered at different temperatures

Figure 4 shows the crystallite size for rutile TiO_2 in $\text{TiO}_2\text{-SiO}_2$ composites with different amounts of TiO_2 , which are sintered at different temperatures. The crystallite size in Figure 4 is for the rutile peak at about $2\theta = 27.3^\circ$ and is calculated using Scherrer's formula (Duy et al., 2014):

$$\langle d \rangle = \frac{0.9\lambda}{\beta \cos \theta} \quad (1)$$

where $\langle d \rangle$ is the mean crystallite size, β is the full width at half maximum in radian, λ is the wavelength of X-ray, and θ is the Bragg angle.

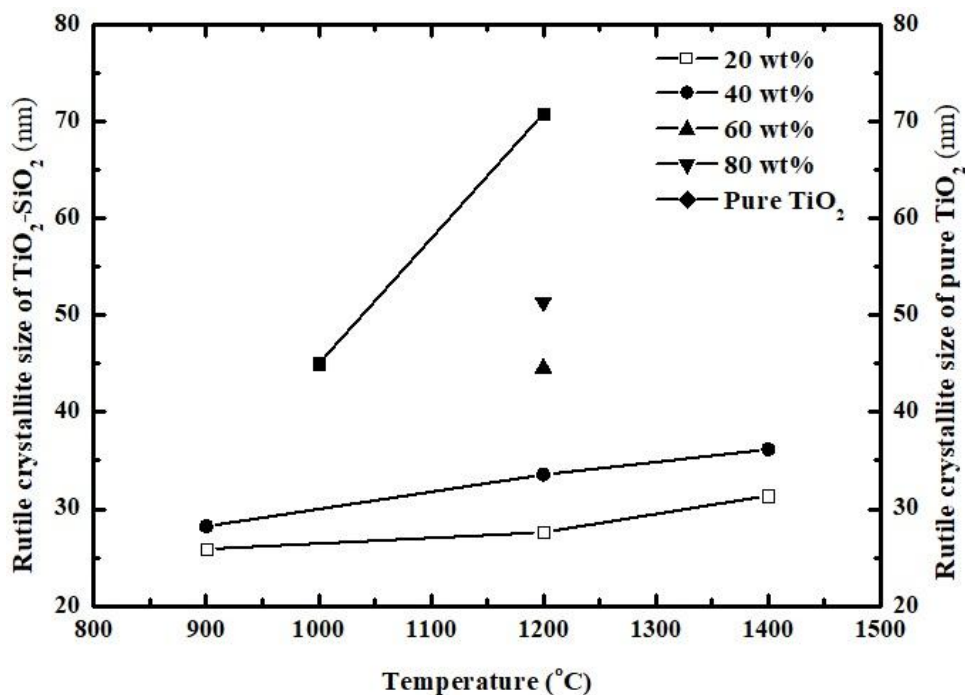


Figure 4 Crystallite size for rutile TiO₂ in TiO₂-SiO₂ composites with different amount of TiO₂, sintered at different temperatures

It is quite obvious from Figure 4 that the gradual increase in temperature from 900°C to 1400°C resulted in the steady enhancement of the rutile crystallite size for the composite samples with 20 wt% and 40 wt% of TiO₂. At 900°C, the crystallite size is 25.86 nm for 20 wt%, while it is only slightly larger, 28.22 nm, for 40 wt%. This result is in agreement with the findings of the study of TiO₂ nanopowders carried out by Chen et al. (2003). Similarly, the increase in TiO₂ content coincided with a steady enhancement in the crystallite size for all composite samples. It was determined that the calculated size of rutile crystallites increases from 27.60 nm to 51.37 nm, when the content of TiO₂ increases from 20 wt% to 80 wt%. In comparison to the results, it was also calculated that the crystallite size for the rutile of pure TiO₂ is 70.81 nm. This means that the crystallite size of rutile can be correlated to the SiO₂ content in the composite; this can be explained as follows. In the case of larger amounts of SiO₂ in the composite, more titania particles are prevented from coming into mutual contact. Thus, the presence of excess SiO₂ has restricted the crystallite growth of TiO₂, thereby delaying the phase conversion from anatase TiO₂ to rutile TiO₂ in the TiO₂-SiO₂ composites. Conversely, for smaller amounts of SiO₂ in the composite, the size of the rutile TiO₂ increases. It is hypothesized that the coarsening of anatase TiO₂ increases when Si atoms are absent (Viswanath & Ramasamy, 1998), and therefore the rate of rapid growth in crystallite size occurs.

Figure 5a shows the FTIR spectra of silica xerogel with varying loading of TiO₂ sintered at 1200°C. For all samples, the absorption bands (peaks 1, 2, and 3) observed at about 464 cm⁻¹, 800 cm⁻¹, and 624 cm⁻¹ were attributed to a Si-O-Si bending vibration, the symmetric stretching mode of the Si-O-Si bond, and the crystalline cristobalite phase, respectively (Wagh & Ingale, 2002; Yang & Gao, 2006). Additionally, for all samples, peak 4, at around 952 cm⁻¹, corresponds to the presence of Si-O-Ti vibration modes, due to the overlapping of the vibration of Si-OH and Si-O-Ti bonds (El-Toni et al., 2006; Balachandaran et al., 2010). From this

observation, one can conclude that silica xerogel chemically binds on the surface of the TiO_2 nanoparticles. The band at 1100 cm^{-1} (peak 5) is attributed to the Si–O–Si bending vibration. Peak 6, observed at 1620 cm^{-1} , is associated with the bending H–O–H bond groups of adsorbed water molecules, while the broad band (peak 7), at 3452 cm^{-1} , is attributed to the O–H stretching of hydroxyl groups that are present on the surface of the material (Yang & Gao, 2006).

Figure 5b shows the integrated intensity for the characteristic band of Si–O–Ti bonds at 952 cm^{-1} for the TiO_2 - SiO_2 composites with different amounts of TiO_2 , sintered at 1200°C . It has been found that the integrated intensity of Si–O–Ti bonds decreases with increasing amounts of TiO_2 . The high quantity of Si–O–Ti bonds with smaller amounts of TiO_2 indicates that more SiO_2 facilitates the aggregation of TiO_2 , and the SiO_2 and TiO_2 phases are not separated from each other in the composite. In this case, the presence of SiO_2 impedes direct contact of TiO_2 particles through Si–O–Ti bonds, resulting in greater suppression of the phase transformation from anatase to rutile. This leads to the formation of smaller particles of rutile TiO_2 with smaller amounts of TiO_2 . It has been confirmed by the XRD patterns that the size of the rutile particles in the sample loaded with larger quantities of SiO_2 is smaller than that of those loaded with smaller quantities of SiO_2 .

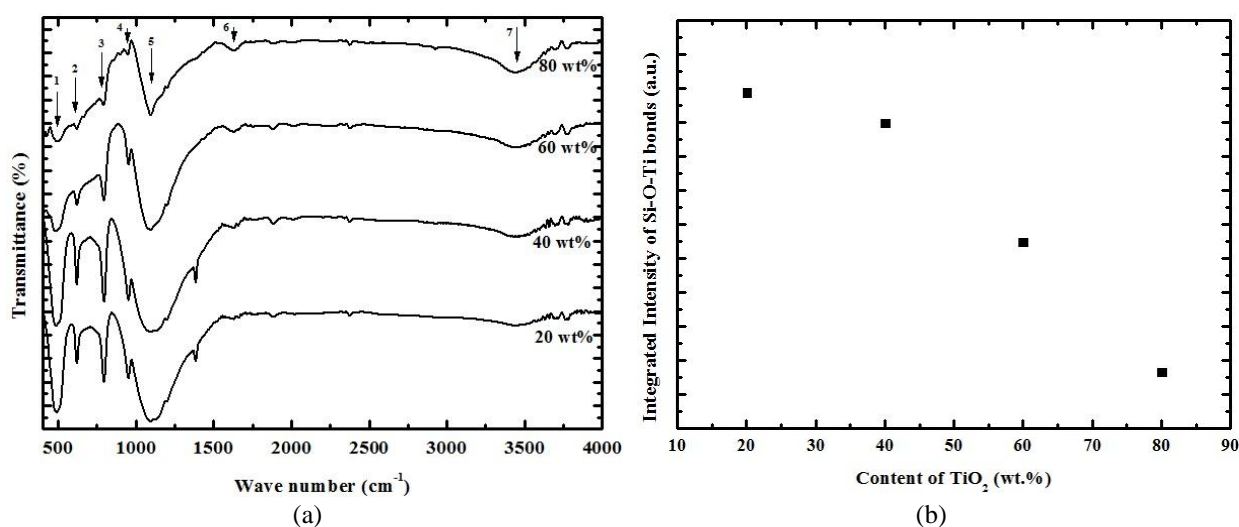


Figure 5 (a) Fourier transform infrared (FTIR) spectra; and (b) Integrated intensity for the characteristic band of Si–O–Ti bonds at 952 cm^{-1} of TiO_2 - SiO_2 composites with different amounts of TiO_2 , sintered at 1200°C

4. CONCLUSION

We have successfully developed a novel composite ceramic by incorporating TiO_2 in silica xerogel converted from sago waste ash. In the experiments, the content of TiO_2 and the sintering temperature have been varied in order to study their influence on the properties of the produced ceramic. The results have confirmed that a complete transformation from the anatase to the rutile TiO_2 phase occurs at 1200°C . A significant effect of SiO_2 on the crystalline growth of rutile TiO_2 is clearly observed at lower concentrations of SiO_2 , a finding which has not been reported before (Aripin et al., 2016). It has also been found that the formation of large quantities of Si–O–Ti bonds results in a significant decrease in the size of rutile crystallites. The results presented in this work show that the incorporation of 20 wt% to 80 wt% TiO_2 into SiO_2 at a temperature of 1200°C causes an appreciable effect on the crystallite size of rutile TiO_2 .

5. ACKNOWLEDGEMENT

This research was supported by a fund of the Siliwangi University through the Project of Research for Guru Besar in 2016 (Contract number: 1140/D3/PL/2016) and was carried out in collaboration with the Nano Technology and Graphene Research Center (NTGRC), Padjadjaran University. The authors would like to thank the research team from the NTGRC for kindly helping to prepare the sintering of the samples.

6. REFERENCES

- Affandi, S., Setyawan, H., Winardi, S., Purwanto, A., Balgis, R., 2009. A Facile Method for Production of High-purity Silica Xerogels from Bagasse Ash. *Advanced Powder Technology*, Volume 20, pp. 468–472
- Aripin, H., Mitsudo, S., Sudiana, I.N., Tani, S., Sako, K., Fujii, Y., Saito, T., Idehara, T., Sabchevski, S., 2011. Rapid Sintering of Silica Xerogel Ceramic Derived from Sago Waste Ash using Sub-millimeter Wave Heating with a 300 GHz CW Gyrotron. *J. Infrared Millimeter and Terahertz Waves*, Volume 32, pp. 867–876
- Aripin, H., Mitsudo, S., Sudiana, I.N., Busaeri, N., Sunendar, B., Sabchevski, S., 2016. Structural Characterization of a Glass Ceramic Developed from TiO₂ and a Novel Material-silica Xerogel Converted from Sago Waste Ash. *Materials Science Forum*, Volume 872, pp. 81–86
- Aripin, H., Mitsudo, S., Prima, E.S., Sudiana, I.N., Tani, S., Sako, K., Fujii, Y., Saito, T., Idehara, T., Sano, S., Sunendar, B., Sabchevski, S., 2012. Structural and Microwave Properties of Silica Xerogel Glass-ceramic Sintered by Sub-millimeter Wave Heating using a Gyrotron. *J. Infrared Millimeter and Terahertz Waves*, Volume 33, pp. 1149–1162
- Aripin, H., Mitsudo, S., Sudiana, I.N., Priatna, E., Kikuchi, H., Sabchevski, S., 2016. Densification Behavior of SnO₂-glass Composites Developed from Silica Xerogel and SnO₂. *International Journal of Technology*, Volume 7(3), pp. 401–440
- Arun, D., Merline Shyla, J., Xavier, F.P., 2012. Synthesis and Characterization of TiO₂/SiO₂ Nano Composites for Solar Cell Applications. *Applied Nanoscience*, Volume 2, pp 429–436
- Aziz, R.A., Sofyan, I., 2009. Synthesis of TiO₂-SiO₂ Powder and Thin Film Photocatalysts by Sol Gel Method. *Indian Journal of Chemistry*, Volume 48A, pp. 951–957
- Balachandaran, K., Venckatesh, R., Sivaraj, R., 2010. Synthesis of Nano TiO₂-SiO₂ Composite using Sol-gel Method: Effect on Size, Surface Morphology and Thermal Stability. *International Journal of Engineering Science and Technology*, Volume 2, pp. 3695–3700
- Chen, Y., Lee, C., Yeng, M., Chiu, H., 2003. The Effect of Calcination Temperature on the Crystallinity of TiO₂ Nanopowders. *Journal of Crystal Growth*, Volume 247, pp. 363–370
- CRC Handbook of Chemistry and Physics, 2006. ed., Lide D.R., Taylor and Francis, Boca Raton, Internet version, Available online at <http://www.hbcnetbase.com>
- Duy, P.P., Kim, K.K., Cao, V.T., Van, Q.V., Thi, T.V., 2014. Preparation and Structural Characterization of Sol-gel-derived Silver Silica Nanocomposite Powders. *International Journal of Materials Science and Applications*, Volume 3, pp. 147–151
- El-Toni, A.M., Yin, S., Sato, T., 2006. Control of Silica Shell Thickness and Microporosity of Titania-silica Core-shell Type Nanoparticles to Depress the Photocatalytic Activity of Titania. *Journal of Colloid and Interface Science*, Volume 300, pp. 123–130
- JCPDS-International Centre for Diffraction Data, 1997. PCPDFWIN: Volume 1.30
- Mahyar, A., Ali Behnajady, M., Modirshahla, N., 2010. Characterization and Photocatalytic Activity of SiO₂-TiO₂ Mixed Oxide Nanoparticles Prepared by Sol Gel Method. *Indian Journal of Chemistry*, Volume 49A, pp. 1593–1600

- Marinela, S., Hyun Choia, D., Heuguet, R., Agrawala, D., Lanagana, M., 2013. Broadband Dielectric Characterization of TiO₂ Ceramics Sintered through Microwave and Conventional Processes. *Ceramics International*, Volume 39, pp. 299–306
- Nilchi, A., Janitabar-Darzi, S., Rasouli-Garmarodi, S., 2011. Sol-gel Preparation of Nanoscale TiO₂/SiO₂ Composite for Eliminating of Con Red Azo Dye. *Materials Sciences and Applications*, Volume 2, pp. 476–480
- Riazian, M., Montazeri, N., Biazar, E., 2011. Nano Structural Properties of TiO₂-SiO₂. *Oriental Journal of Chemistry*, Volume 27, pp. 907–910
- Shumaila, I., Rahman, R.A., Riaz, S., Naseem, S., Othaman, Z., Saeed, M.A., 2015. High Surface Area SiO₂-TiO₂ Nano-composite as pH Sensor. *Sensor and Actuator B: Chemical*, Volume 221, pp. 993–1002
- Syahrial, A.Z., Priyono, B., Yuwono, A.H., Kartini, E., Jodi, H., Johansyah, 2016. Synthesis of Lithium Titanate (Li₄Ti₅O₁₂) by Addition of Excess Lithium Carbonate (Li₂CO₃) in Titanium Dioxide (TiO₂) Xerogel. *International Journal of Technology*, Volume 7(3), pp. 392–400
- Vishwas, M., Narasimha Rao, K., Arjuna Gowda, K.V., Chakradhar, R.P.S., 2011. Optical, Electrical and Dielectric Properties of TiO₂-SiO₂ Films Prepared by a Cost Effective Sol-gel Process. *Spectrochimica Acta Part A*, Volume 83, pp. 614–617
- Viswanath, R.N., Ramasamy, S., 1998. Study of TiO₂ Nanocrystalline in TiO₂-SiO₂ Composites. *Colloid and Surface A*, Volume 133, pp. 49–56
- Wagh, P.B., Ingale, S.V., 2002. Comparison of Some Physico-chemical Properties of Hydrophilic and Hydrophobic Silica Aerogels. *Ceramic International*, Volume 28, pp. 43–50
- Wang, X., Masumoto, H., Someno, Y., Hirai, T., 1999. Microstructure and Optical Properties of Amorphous TiO₂-SiO₂ Composite Films Synthesized by Helicon Plasma Sputtering. *Thin Solid Films*, Volume 338, pp.105–110
- Xue, S.H., Xie, H., Ping, H., Li, Q., Su, B., Fu, Z., 2015. Induced Transformation of Amorphous Silica to Cristobalite on Bacterial Surfaces. *RSC Advances*, Volume 5, pp. 71844–71848
- Yang, L., Lai, Y., Chen, J.S., Tsai, P.H., 2005. Compositional Tailored Sol-Gel SiO₂-TiO₂ Thin Films: Crystallization, Chemical Bonding Configuration, and Optical Properties. *Journal of Material Research*, Volume 20, pp. 3141–3149
- Yang, S., Gao, L., 2006. Facile and Surfactant-free Route to Nanocrystalline Mesoporous Tin Oxide. *Journal of the American Ceramic Society*, Volume 89, pp. 1742–1744
- Yuwono, A.H., Zhang, Y., Wang, J., 2010. Investigating the Nanostructural Evolution of TiO₂ Nanoparticles in the Sol-gel Derived TiO₂-Polymethyl Methacrylate Nanocomposites. *International Journal of Technology*, Volume 1(1), pp. 11–19